Parametric models for WEC performances

Parametric models for WEC performances

Rémy Pascal
Institute for Energy System,
The University of Edinburgh, UK
E-mail: remy.pascal@ed.ac.uk

Grégory Payne
Institute for Energy System,
The University of Edinburgh, UK
E-mail: gregory.payne@ed.ac.uk

Ian Bryden
Institute for Energy System,
The University of Edinburgh, UK
E-mail: ian.bryden@ed.ac.uk

***Abstract*—Wave energy is an emerging and promising renewable energy technology. As the first pre-commercial and commercial prototypes are being tested at sea, there is a need for developers, governments and investors to be able to reliably estimate the energy production of devices as a function of the sea states they are to be deployed in. This estimate has traditionally relied on only two sea state parameters, the significant wave height and the energy period, which do not account for frequency or directional spreading. The present paper investigates the suitability of further parameters to refine performance predictions. This is achieved through extensive wave tank testing of three types of wave energy converters (WECs) with different directionality properties. Statistical analyses of the measurements show the significant impact of frequency and directional spreading on WECs performance. Parametric models of the devices performances were devised for numerous sea states parameters. Those results suggest that the traditional estimation method should be extended in order to include such parameters.**

***Index Terms*—performance prediction, WEC, parametric models, tank testing, uni-modal spectra.**

I. Introduction

Predicting the energy production of Wave Energy Converters (WECs) at a given location is an important need of the wave energy industry. However, it is still an uncertain process [1] due to the difficulty of statistically describing wave climates and to combine these statistical data with performance characteristics of WECs.

Reducing a sea state to its directional spectrum is a widespread approach despite the fact that this method does not account for the relative phases between waves. Directional wave data are available from numerous locations, and statistical analyses are carried out to try to characterise the corresponding wave climate. However, as their influence over the performance of WECs is not always well understood, little is still used of those statistics. For many performance predictions, the only statistical quantities taken into account are the significant wave height H_{m0} and energy period T_E which are used to generate a scatter diagram which is in turn combined with the power matrix of a device to predict performance.

During the EWTEC 2009, a project was presented aiming at quantifying the influence of several directional spectral parameters over the performance of different WECs [2]. This paper presents the findings related to the measurements of uni-modal spectra. The influence of the spectral shape on the performance of three types of WECs is investigated and compared to the influence of the energy period.

II. Sea state parameters and test plan

A. The devices

The WEC models selected for this project had to satisfy multiple goals. Primary, they should represent a broad range of WEC concepts for the results to be as generic as possible. Second, the comparison of the effect of directional spectrum parameters on directional and omnidirectional devices is of particular interest, so the chosen devices must range from purely omnidirectional (mooring included) to strongly directional. Finally, the Edinburgh Curved tank can only accommodate deep water devices, and reliable models from prior work were favoured as this project is not focused on developing new models.

Aside of those constraints, outstanding performances are not required for those models. As the main goal is to study their performance variation relative to the spectral parameters, absolute performance is not a strong concern, and emphasis is put on the repeatability and precision of the performance measurements.

The three WEC models chosen according the above constraints are the followings:

- A single fixed Oscillating Water Column (OWC) model. The model utilised was developed by Queen's University Belfast, so it has been tested and validated before being used in this study. The single fixed OWC is a generic omnidirectional device. It is expected that it will not be affected by the effect of wave directionality.
- Two fixed OWCs (see Fig. 1). They are two identical instances of the previous model. By being considered as a single device, the two OWCs are standing for a weakly directional device that cannot align itself with the main wave direction of propagation.
- The desalination duck model (see Fig. 2). This model is an evolution of the Edinburgh Duck and it has been developed and tested continuously at the University of Edinburgh during the last four years [3], [4], [5] and [6]. The desalination duck model is a fully directional device that can align itself with the waves.

B. Parameters

To investigate the spectral shape of uni-modal spectra, a frequency spreading parameters f_s and an angular spreading parameter Θ_S were used. The possibility of variation in the mean direction of propagation $\theta_{mean}(f)$ with respect

TABLE I
LIST OF SEA STATE PARAMETERS.

Symbol	Physical meaning	Unit	Equation
H_{m0}	significant wave height	m	$H_{m0} = 4\sqrt{m_0}$
T_E	energy period	s	$T_E = \frac{m_{-1}}{m_0}$
$\theta_{mean,p}$	mean direction at each frequency	deg(°)	$\theta_{mean,p} = \frac{\sum_q S_{f_p,\theta_q}\theta_q}{\sum_q S_{f_p,\theta_q}}$
$\delta\theta_m$	variation of $\theta_{mean,p}$ along the frequency axis	deg(°)/Hz	coefficient of the linear regression of $\theta_{mean,p}$ as a function of the frequency.
Θ_M	integrated mean direction over the frequencies	deg(°)	$\Theta_M = \frac{\sum_p S_{f_p}\theta_{mean,p}}{\sum_p S_{f_p}}$
f_s	frequency spreading parameter	Hz	$f_s^2 = \frac{\sum_p S_{f_p}(f_p - \frac{1}{T_E})^2}{\sum_p S_{f_p}}$
θ_{sp}	angular spreading factor at each frequency	deg(°)	$\theta_{sp}^2 = \frac{\sum_q S_{f_p,\theta_q}(\theta_q - \theta_{mean,p})^2}{\sum_q S_{f_p,\theta_q}}$
Θ_S	the integrated angular spreading factor	deg(°)	$\Theta_S = \frac{\sum_p S_{f_p}\theta_{sp}}{\sum_p S_{f_p}}$

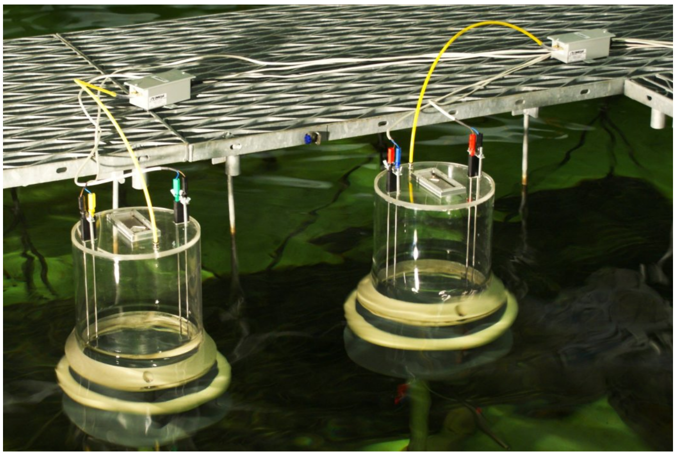

Fig. 1. Photo of the double OWC during the measurements.

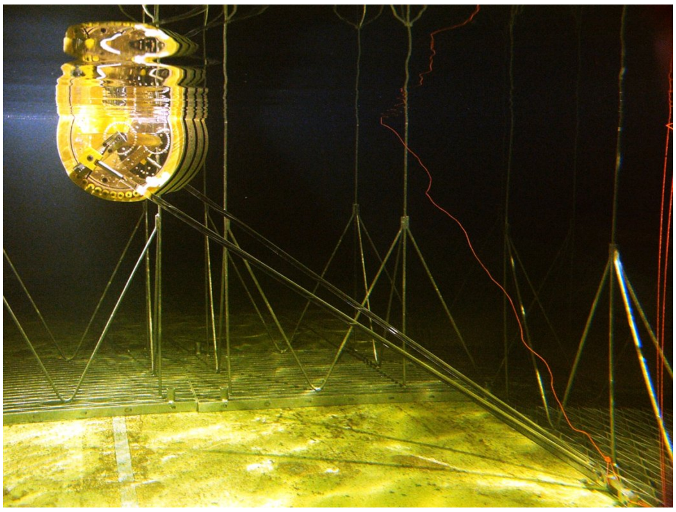

Fig. 2. Underwater photo of the desalination duck model moored in the Edinburgh Curved Wave tank.

to frequency was also considered: $\delta\theta_M$ is defined as the coefficient of the linear regression fitted to the observed values of $\theta_{mean}(f)$. The influence of each parameters will be compared with the influence of the energy period T_E. The mathematical definitions of those and other relevant parameters are given in Table I.
Numerous parameters related to the width of omnidirectional frequency spectra have been proposed in the past. An extensive list was presented by [7], as well as a first study of the correlation between such parameters and the performances of wave energy converters. There is currently no widespread consensus on how relevant these parameters are with respect to each other. The decision was made to use f_s as its physical meaning is obvious. It is the weighted average of the distance to the energy frequency. Fig. 3 shows the evolution of f_s with γ, the peak enhancement parameter in the JONSWAP formula.

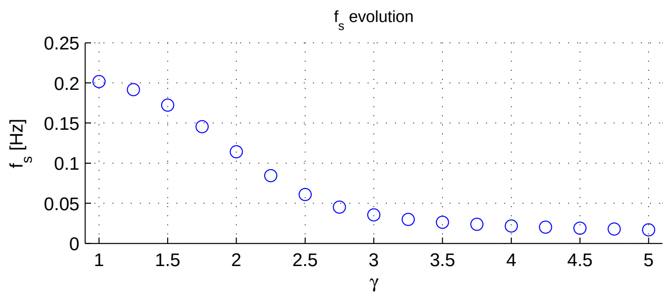

Fig. 3. f_s as a function of γ the peak enhancment parameter of JONSWAP spectra.

It shows that f_s is a very discriminant parameter for values of γ between 0 and 3.3. Fortunately, those are the values commonly used ($\gamma = 1$ corresponds to a Bretschneider spectrum, and $\gamma = 3.3$ is the standard value for JONSWAP [8]). A clear distinction between the frequency spreading values of the wave systems generated in the tank is expected. f_s should consequently be adequate to be used in this work. In order to reduce the number of tests required, some important parameters are not considered. H_{m0} is not used. Its influence on WECs performances is not put into question, and it is not anticipated that it will have significant interaction with other parameters. Hence little additional knowledge would be gain by including it in the study. The mean direction of propagation Θ_M will also not be investigated. Most deep water devices are either omnidirectional or they can align themselves with the mean direction of propagation.

C. Test plan

The test plan should allow the evaluation of the effect of each parameters and the interactions between them. A full factorial design is devised to achieve this.
It is widely acknowledged that the relationship between T_E and the energy production of resonating WECs is not linear. In consequence, the tests will investigate three values of T_E. For the other three parameters, only two values are used in order to minimize the number of combinations. The two values of f_s are generated by utilising two different *Types* of spectral shape: JONSWAP and Bretschneider. The angular spreading values are modelled with a $\cos^{2s}$ spreading function. s values of 5 and 100 are used. The two levels of $\delta\theta_{m,1}$ are achieved by varying $\tau_n = |\theta_{mean,max} - \theta_{mean,min}|$, expressed in degrees. The mean directions $\theta_{mean,p}$ of each frequency bands p (see [9]) are linearly set between the values taken by $\theta_{mean,max}$ and $\theta_{mean,max}$. The parameter τ_n is thus directly linked to $\delta\theta_{m,n}$.
Altogether, this amounts to 24 combinations. Five runs with different random phase spectra are used for each combination, which leads to 120 different sea states. As three models are considered and adding the dry runs needed to measure the waves, a full factorial design needs 480 individuals measurements of $1024\,\mathrm{s}$, roughly amounting to $150\,\mathrm{h}$ of tests. This is considered to be to upper limit of what is manageable within the scope of this study. The list of sea states is described in Table II.

TABLE II
LIST OF SEA STATE USED UNI-MODAL TESTS.

Sea State	T_E	τ_n	Θ_S	Spectral shape
seaState 1	0.83	0	small	Bretschneider
seaState 2	0.83	0	small	JONSWAP
seaState 3	0.83	0	large	Bretschneider
seaState 4	0.83	0	large	JONSWAP
seaState 5	0.83	20	small	Bretschneider
seaState 6	0.83	20	small	JONSWAP
seaState 7	0.83	20	large	Bretschneider
seaState 8	0.83	20	large	JONSWAP
seaState 9	1	0	small	Bretschneider
seaState 10	1	0	small	JONSWAP
seaState 11	1	0	large	Bretschneider
seaState 12	1	0	large	JONSWAP
seaState 13	1	20	small	Bretschneider
seaState 14	1	20	small	JONSWAP
seaState 15	1	20	large	Bretschneider
seaState 16	1	20	large	JONSWAP
seaState 17	1.14	0	small	Bretschneider
seaState 18	1.14	0	small	JONSWAP
seaState 19	1.14	0	large	Bretschneider
seaState 20	1.14	0	large	JONSWAP
seaState 21	1.14	20	small	Bretschneider
seaState 22	1.14	20	small	JONSWAP
seaState 23	1.14	20	large	Bretschneider
seaState 24	1.14	20	large	JONSWAP

D. Sea states measurements

Measuring those sea states is essential. The calibration of the Edinburgh Curved Tank is not fully established as no practical mean of refining it is available. Hence, differences between target and estimated values can find their cause either in the sea state estimation method inaccuracies or in the waves actually generated by the tank.
Records of $1024\,\mathrm{s}$ with a sampling frequency of $16\,\mathrm{Hz}$ were taken for each run. It corresponds for a full repeat period of each sea state and yields a frequncy resolution of $\simeq 0.00098\,\mathrm{Hz}$. The Nyquist frequency is $8\,\mathrm{Hz}$ which is considered high enough given that the frequency of the shortest waves generated $1.75\,\mathrm{Hz}$.
The method used to obtain spectra estimate of sea states in the tank is described in [9]. It is a version of the Maximum Likelihood Method (MLM) adapted to the deterministic nature of the waves generated in the Edinburgh Curved Tank. As the research project also included bi-modal spectra, a wave system isolation routine was developed. The routine works as follows. For a given point of the (f, θ) energy spectrum, the gradient vector of the spectrum at that point is computed. The decision of whether to include that point in the wave system is based on the magnitude of the gradient vector and on its direction. The point is more likely to be included in the wave system if the gradient vector points towards the peak of the system and if the vector magnitude is high. A complete description of the routine can be found in [9]. Using this routine, sea state parameters can be computed either with respect to the full spectra or only with respect to the isolated wave system. When parameters are estimated with respect to the wave system only, the same mathematical expressions as in Table I are used but the spectral estimates outside of the isolated system are set to 0. Sea states parameters estimated with respect to a wave system are thus robust to the presence of noise in the spectral estimate. When a parameters is estimated with respect to a wave system, it is noted with an extra subscript relative to the wave system: T_E becomes $T_{E,1}$. The distinction between estimates and target values is marked by a $\hat{}$ on top of the estimated values.
The plots presented in this paper include parameters estimated after isolation (*estimated isolated*), as well as parameters computed from the target spectra but using the boundaries of the system defined by the isolation routines (*target isolated*). The latter set of measurements provides an indication of the performances of the isolation routine.

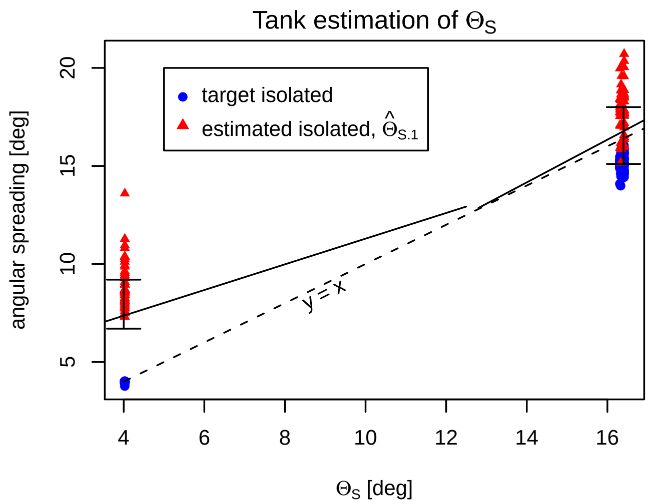

Fig. 4. Graph relating the observed $\hat{\Theta}_{S,1}$ in the tank and Θ_S. The solid line is a reminder of the model estimated from virtual data presented in [9]. The bars represent the scatter observed in the virtual data test. The dash lines represent the ideal case where observed and target values match entirely.

1) Measurement of Θ_S*:* Fig. 4 shows the estimated isolated $\hat{\Theta}_{S,1}$ and the target isolated $\Theta_{S,1}$ plotted against Θ_S. The first observation is that the isolation technique is effective. The estimated values are slightly larger than expected from the virtual tests and with more scatter. The virtual and real wave measurements have been obtained using the same generation method, the same estimation routine and identical wave gauge layout. The discrepancies have therefore to be explained either by the inadequacy of the virtual wave elevation, or by variations in the spectra. Given that the results are mainly sensitive to the level of reflection and that the 10% included in the virtual data can be considered as conservative (see [10]), it is believed that the differences observed reflects real variations of the generated spectra. The tank calibration used during those tests is the first possible cause. As the level of angular spreading is shown to vary more than expected, it is difficult to treat $\hat{\Theta}_{S,1}$ as a bi-level factor. In the subsequent data analysis, it will be introduced as a continuous variable.

2) Measurement of H_{m0}*:* While H_{m0} is not one of the considered parameters, it is important to monitor its variation from sea states to sea states. It appears that clipping of the high frequencies at 1.75 Hz, inaccuracies of the tank calibration and influence of the isolation routine introduce variations in H_{m0} with respect to the *Type* of spectra, to T_E and to the angular spreading.

H_{m0} is not specifically a directional parameter, so for uni-modal spectra one should be able to use an estimate of either H_{m0} or $H_{m0,1}$. However, selecting the right estimator for the significant wave height is problematic. The summary of the values observed in the tank given in Fig. 5 shows that none of the two estimates is entirely satisfying. Correlations between estimates of H_{m0} and other values can be observed:

- A negative correlation is observed between $\hat{H}_{m0}$ and T_E while there is a positive relation between the *target isolated* values of H_{m0} and T_E. The same trends can be observed with respect to $\hat{T}_{E,1}$. In both cases, $\hat{H}_{m0,1}$ appears to be decoupled from the energy period estimates. This suggests that $\hat{H}_{m0,1}$ should be the most relevant estimator for the significant wave height.
- A correlation between the significant wave height estimators and $\hat{\Theta}_{S,1}$ is expected from the test with virtual waves. In the tank experiment, $\hat{H}_{m0}$ and $\hat{H}_{m0,1}$ exhibit similar trends pointing towards higher significant wave height for broader spectra. This is thought to be the results of both the influence of the isolation routine and of the tank calibration.

The examination of the correlation defines $\hat{H}_{m0,1}$ as the most appropriate estimate. Also, $\hat{H}_{m0}$ does not separate incident and reflected spectra, which might be an issue while analysing the results from a directional sensitive device. However, $\hat{H}_{m0,1}$ values are low compared to $\hat{H}_{m0}$ ($\sim$ 60%), which would leads to higher than expected estimations of capture width in comparison with previous published studies. Finally, $\hat{H}_{m0,1}$ will be used for the performance analysis of the devices in order to avoid the correlation with $\hat{T}_E$.

3) Measurement of f_s*:* Fig. 6 shows $\hat{f}_{s,1}$ as a function of f_s. The experimental values are fitting relatively well with the model from the virtual wave testing, so there is no particular concern here. Despite the scatter in the data, it is possible to make a clear distinction between the two types of spectra, JONSWAP and Bretschneider. At this stage, it is not clear if the scatter in the data really represents variation of f_s for the same type of spectra or if it is only an artefact of the measurement method. Alternative models using either the continuous variable $\hat{f}_{s,1}$ or the bi-level factor *Type* will be used in the subsequent device performance analysis, and a final decision will be made on comparing which model fits best the data.

4) Other parameters: The energy period measures are unsurprising. The values are slightly higher than expected, which can probably be explained by the clipping of the spectra highest frequencies. $\hat{T}_{E,1}$ will be used to evaluate the performances of the devices for consistency reasons with $\hat{H}_{m0,1}$.

Measurements of $\delta\theta_m$ are not satisfactory. A significant amount of scatter has been observed. It would be surprising if the devices measurements would allow to identify any effect of $\delta\theta_m$ over the WEC models' performances.

III. Device Results

A. Retained performance indicators

The normalised power P^n is selected as the performance indicator for the devices. It allows a fair comparison between

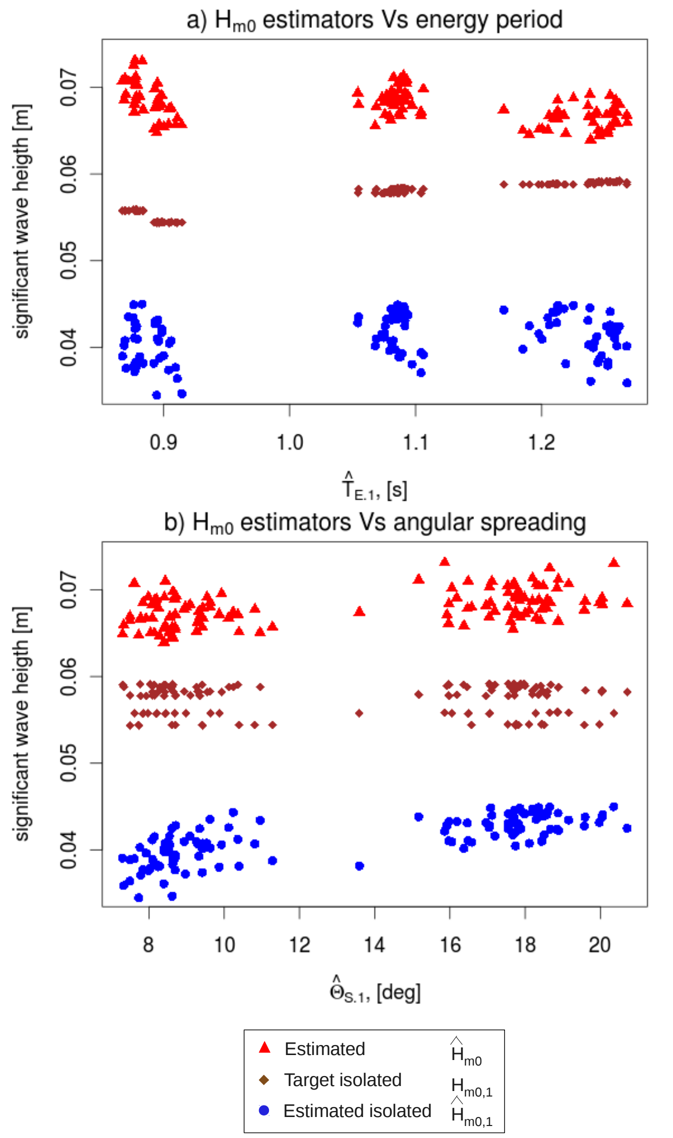

Fig. 5. Significant wave height measures during the first phase tests as a function of the relevant spectrum parameters.

the devices. P^n is computed as described in Eq. 1:

$$P^n = \frac{\overline{P}}{\max\limits_{i}\left(\frac{\sum_j \overline{P_{i,j}}}{runs_i}\right)} \tag{1}$$

with: $i \in (1, seastates),\ j \in (1, runs_i)$

$runs_i =$ number of recorded runs for sea state i

$\overline{P} =$ average power output during a run

Due to its formulation, the normalised power P^n can actually take values above 1 as it is not normalised by the maximum observed average power produced by the device but by the observed maximum of the average over the runs for each sea states.

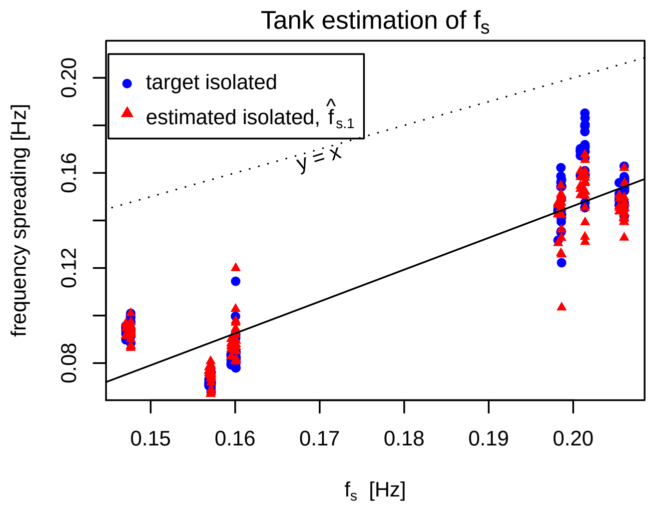

Fig. 6. Graph relating the observed $\hat{f}_{s,1}$ in the tank and f_s. The solid line is a representation of the model devised with simulated data in [10]. The dash line represents the ideal case where observed and target values match.

B. Individual test results

1) Single OWC results: Two runs over the 120 recorded for the single OWC presented power outputs far above the rest and were therefore discarded. The following results are consequently built over 118 measures.

Fig. 7 shows the variation observed between each of the five runs. Outputs for each run are very similar, and there is little concern about the repeatability of the measurements. This observation is creditable to the quality of the wave generated in the curved tank, and it confirms that the phase spectra do not have a strong influence over the OWC performances. Fig. 8 shows the variation of P^n with respect to the main sea

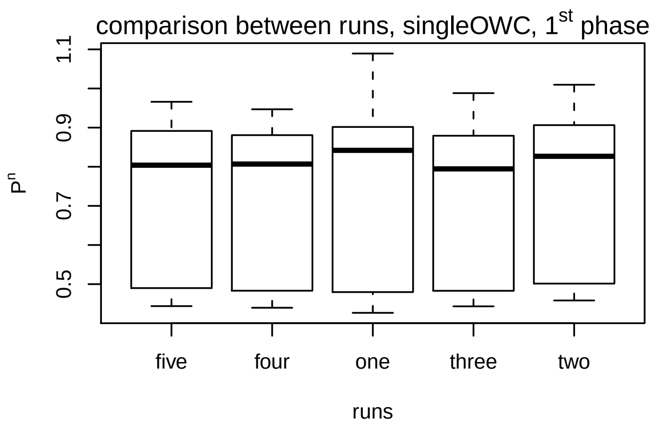

Fig. 7. Variation of P^n as a function of each run for the single OWC.

state parameters. Results from JONSWAP and Bretschneider spectra were differentiated in order to get a better view of the interaction between f_s and the other parameters. The interaction parameter $\hat{T}_{E,1} \cdot \hat{f}_{s,1}$ is included.

A strong correlation with $T_{E,1}$ is obvious with some degree of non-linearity. $f_{s,1}$ seems to also have a strong influence on the

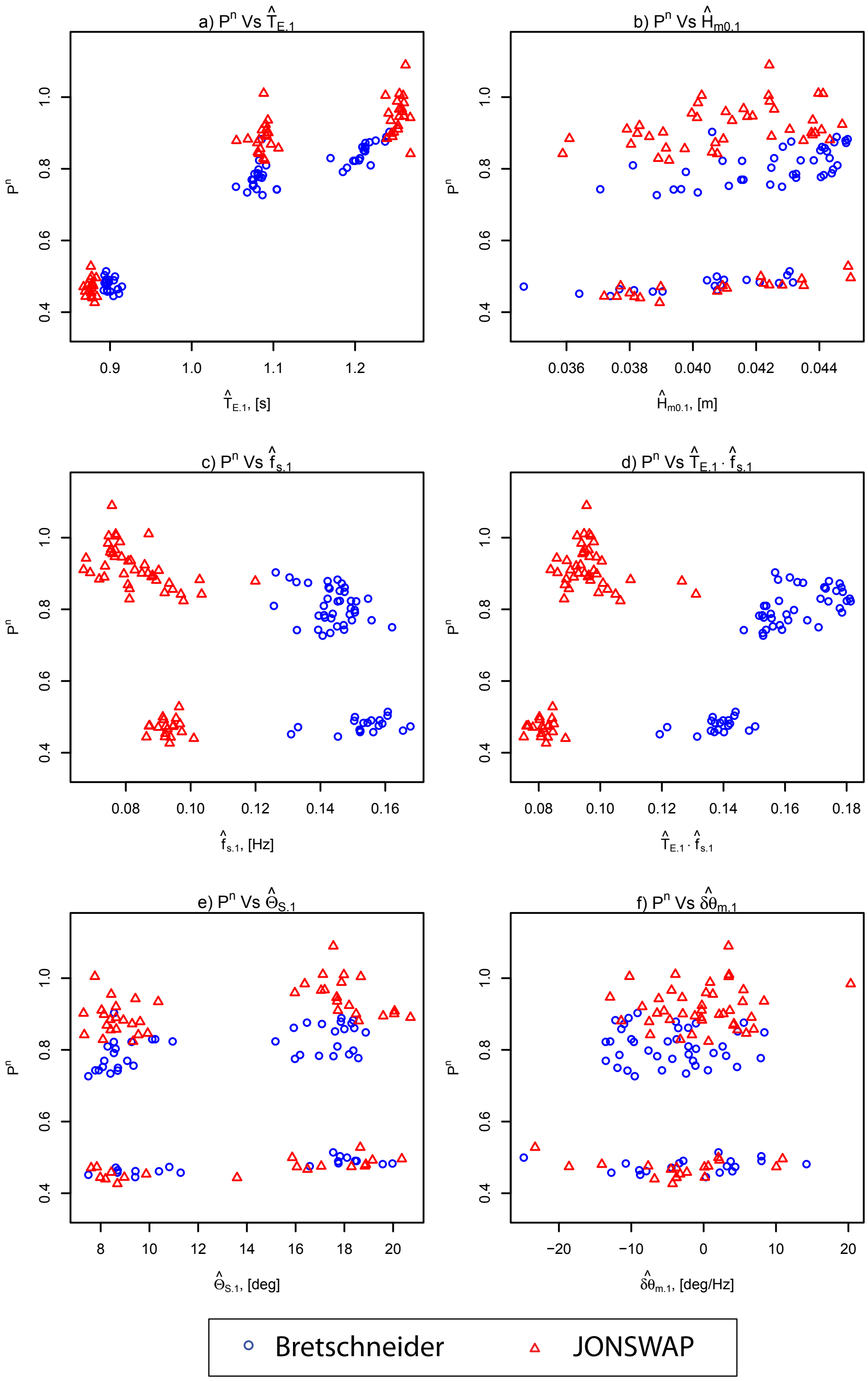

Fig. 8. Variation of P^n as a function of the sea state parameters for the single OWC

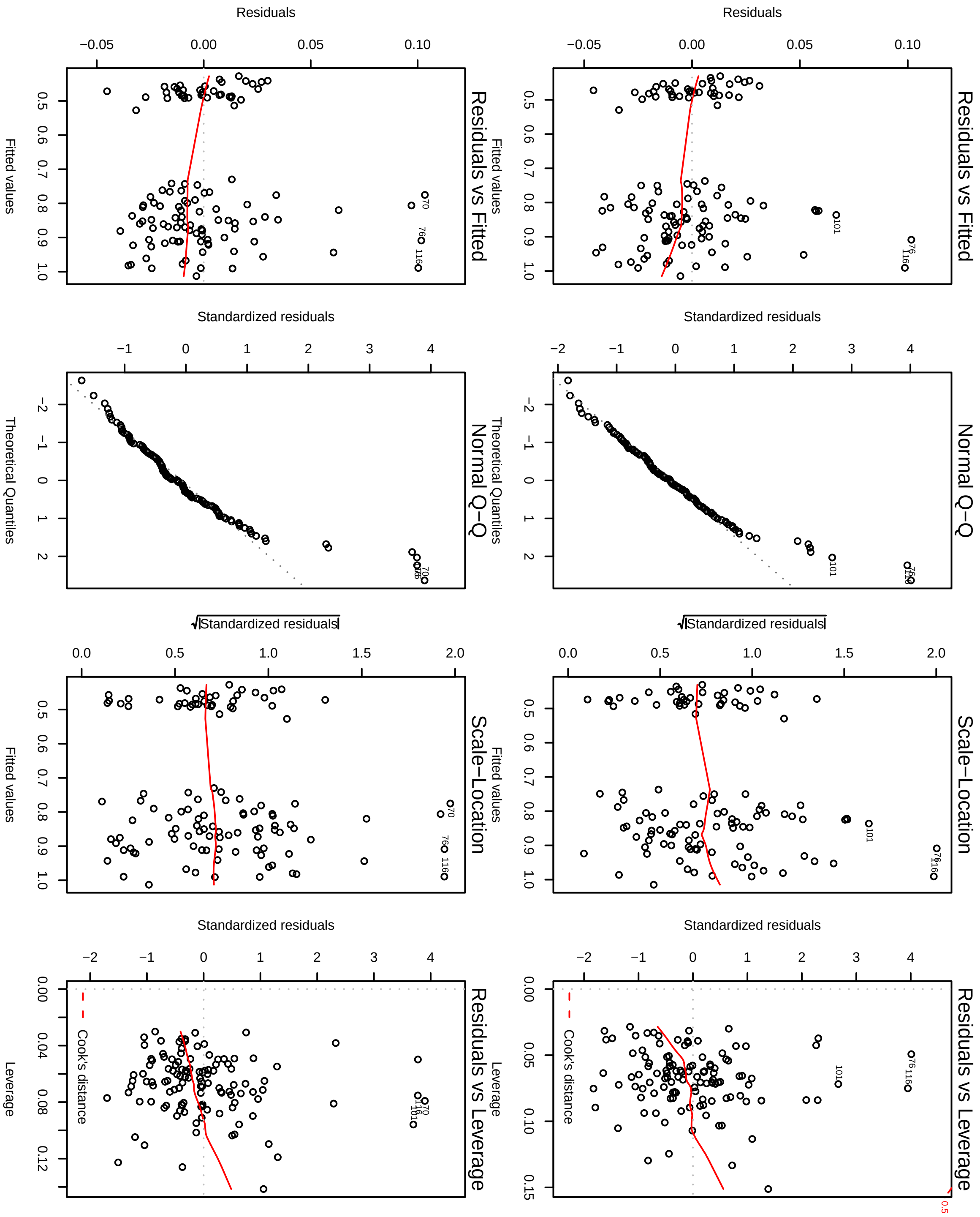

Fig. 9. Test plots to evaluate the fit of the P^n models for the single OWC. Plots related to $PnModel1$ are in the top row, plots related to $PnModel2$ are in the bottom row. Rows refers to the figure observed in landscape orientation.

observed results, both as a single parameters and in interaction with the others. On the contrary, $\delta\theta_{m,1}$ do not seem to have a strong influence on the results as it was expected.

A positive trend can be observed on graphs b) and e) of Fig. 8. It is particularly visible for the group formed by the lower values of P^n. However, some positive correlation was identified between $\hat{H}_{m0,1}$ and $\hat{\Theta}_{S,1}$. Based only on those graphs, it is consequently impossible to conclude which parameter the normalised power is sensitive to.

Using the statistical language *R* (see [11] and [12]), multi-linear regression models are fit to the observed data using either $\hat{f}_{s,1}$ or a bi-level categorical factor *Type* to include the frequency spreading. A $\hat{T}^2_{E,1}$ is introduced to take into account the observed curvature along the energy period axis. The second order interaction between the main factors are also included. The definition of both models is presented in Eq. 2 and Eq. 3:

$$PnModel1 \leftarrow lm\left(P^n \sim \hat{T}_{E,1}{}^2 + \hat{H}_{m0,1} + (\hat{T}_{E,1} + \hat{f}_{s,1} + \hat{\Theta}_{S,1} + \hat{\delta\theta}_{m,1})^2\right) \quad (2)$$

$$PnModel2 \leftarrow lm\left(P^n \sim \hat{T}_{E,1}{}^2 + \hat{H}_{m0,1} + (\hat{T}_{E,1} + Type + \hat{\Theta}_{S,1} + \hat{\delta\theta}_{m,1})^2\right) \quad (3)$$

Each model is then simplified to reach its associated *minimal adequate model*. The fit of the models is evaluated with the standard set of plots provided by *R*. They are presented together in Fig. 9. Both models offer a relatively good fit. (max residuals $\approx 10\%$ and most $< 4\%$). In all cases, the highest residual are too high to be properly normaly distributed, but the majority of points are.

The *Normal Q-Q* plots are better in the model using the continuous variable $\hat{f}_{s,1}$ rather than the bi-level factor $Type$. It gives credit to the hypothesis that at least part of the variation in $\hat{f}_{s,1}$ is due to real features of the generated waves, and not only due to the isolation method. $\hat{f}_{s,1}$ will consequently be utilised for any further models. None of the points presenting larger errors was singled out as highly influential in the *Residuals vs Leverage* plots, so they are not excluded from the models.

The *minimal adequate model* derived from $PnModel1$ is presented in Eq. 4.

$$P^n = -(5.39 \pm 0.22) + (9.35 \pm 0.40) \cdot \hat{T}_{E,1} - (3.70 \pm 0.18) \cdot \hat{T}_{E,1}{}^2 + (15.11 \pm 1.98) \cdot \hat{H}_{m0,1} + (3.50 \pm 0.63) \cdot \hat{f}_{s,1} - (0.014 \pm 0.004) \cdot \hat{\Theta}_{S,1} - (4.73 \pm 0.60) \cdot \hat{T}_{E,1} \cdot \hat{f}_{s,1} + (0.012 \pm 0.004) \cdot \hat{T}_{E,1} \cdot \hat{\Theta}_{S,1} \quad (4)$$

Only $\delta\theta_{m,1}$ is not retained as a significant parameter. The estimated angular spreading $\hat{\Theta}_{S,1}$ is kept as significant. A similar pattern is observed for both spreading parameters. A negative coefficient is attributed to the parameters themselves, but a positive coefficient of similar magnitude is attributed to their interaction with $\hat{T}_{E,1}$.

2) Double OWC results: As the OWCs had to be sent back to Queen's University Belfast at the end of June, only 4 runs for each sea state could be recorded for the double OWC. Additionally, it appears during the data analysis that some records were not satisfactory and had to be discarded. This reduced the number of usable measures from 120 planned to only 84. While the number of test is still significant, it may lead to larger error on the estimation of the coefficients and the significance of parameters effects will be more difficult to assess.

The observations of the double OWC power output with respect to each sea state parameter are similar to those of the single OWC. They are therefore not shown in this paper. The same data analysis method is applied to the results, using only $\hat{f}_{s,1}$ as an estimator for the frequency spreading. The resulting *minimal adequate model* fitted to the data is presented in Eq. 5:

$$P^n = -(5.33 \pm 0.24) + (9.61 \pm 0.43) \cdot \hat{T}_{E,1} - (3.70 \pm 0.19) \cdot \hat{T}_{E,1}{}^2 + (5.73 \pm 1.15) \cdot \hat{H}_{m0,1} + (3.14 \pm 0.66) \cdot \hat{f}_{s,1} - (4.17 \pm 0.62) \cdot \hat{T}_{E,1} \cdot \hat{f}_{s,1} \quad (5)$$

This model is simpler than the one achieved for the single OWC. $\hat{\Theta}_{S,1}$ was not retained as a significant parameter. This is surprising, as the double OWC should have been more sensitive to wave directionality than the single OWC. It is possible that the reduced number of tests did not make it possible to identify the effect of $\hat{\Theta}_{S,1}$. Most probably, the effect of $\hat{\Theta}_{S,1}$ in the single OWC case is resulting from its interaction with $\hat{H}_{m0,1}$. More tests, with a better controlled $\hat{H}_{m0,1}$ would be necessary to clearly separate both effects.

3) Duck results: For this device, only 90 runs could be exploited. The model performances were inferred from pitch motion rather than pressure measurements because of a faulty pressure sensor. No less than 3 runs per sea states were successfully recorded.

The Duck results are similar to those of the OWCs, but no curvature with respect to $\hat{T}_{E,1}$ can be observed. This is probably due to the lower resonance frequency of the model compared to the OWCs. As for the double OWC, only the *minimal adequate model* resulting from the multi-linear analysis is presented in Eq. 6:

$$P^n = -(2.16 \pm 0.27) + (2.23 \pm 0.17) \cdot \hat{T}_{E,1} + (12.38 \pm 4.52) \cdot \hat{H}_{m0,1} + (3.46 \pm 1.60) \cdot \hat{f}_{s,1} - (0.007 \pm 0.002) \cdot \hat{\Theta}_{S,1} - (3.69 \pm 1.50) \cdot \hat{T}_{E,1} \cdot \hat{f}_{s,1} \quad (6)$$

As for the previous devices, the frequency spreading and its interaction with the energy period is retained in the minimal adequate model. The angular spreading is also retained with a negative coefficient despite the smaller number of tests. In contrast with the observations for the single OWC, this could be an indication of its influence.

IV. Conclusions

Tank tests of three devices were conducted in the Edinburgh Curved tank in order to assess the influence of several directional sea states parameters. Those parameters are the energy period, the frequency spreading, the angular spreading and a variation of the mean direction of propagation. The devices are: a single OWC rigidly mounted to the sea bed, a pair of

OWCs and a model of the desalination Duck. A set of of 24 sea states was devised. The generated sea states were estimated with a version of the maximum likelihood method adapted to the deterministic nature of the generated waves.

The results of the sea states estimation show that the energy period, the frequency spreading and the angular spreading were accurate enough for the test. However, the variation of the mean direction of propagation exhibited too much scatter. Additionally, variations of the significant wave height were observed between the sea states and the significant wave height had to be included in the analysis of the devices power outputs. Using statistical analysis, parametric models of the devices performances were devised. Those models are only valid for the parameters range explored but it demonstrates that such models are possible. The effect of the frequency spreading and its interaction with the energy period has been shown to be significant for the results of the three devices. This calls into question the common practice which is relying only on the energy period and the significant wave height for performance prediction of wave energy devices.

V. Future work

The quantification of the effect identified as significant is underway. It would help deciding which parameters are dominant and essential to be considered for performance prediction of WECs. The devised parametric models should be put to test with different spectral shapes. First, spectra with parameters inside the range of parameters used to define the parametric models and with random spectral shape should be used. If the parametric models are effective at estimating the power absorbed by the devices in those sea states, a second group of sea states could be used to explore to which extent the parametric models could be extrapolated to sea states with parameters outside the explored range of parameters.

The parametric models could then be further improved with a new serie of tests. The significant wave height would be integrated in the new test plan, ensuring that its variations are not correlated with other relevant parameters.

Acknowledgment

The authors acknowledges the support of the EPSRC SuperGen Marine programme.

References

[1] B. Holmes and S. Barrett, "Sea & Swell Spectra," in *Proceedings of the 7th European Wave and Tidal Energy Conference*, Porto, Portugal, Sep. 2007.

[2] R. Pascal and I. Bryden, "Toward reliable production estimation from Wave Energy Converters," in *Proceedings of the 8th European Wave and Tidal Energy Conference*, Uppsala, Sweden, Sep. 2009, pp. 1–8.

[3] R. Pascal, "Wave quality assessment and Testing of a Wave Energy Converter in the Edinburgh Curved Wave Tank," master thesis, Chalmers University of Technology, 2006.

[4] S. H. Salter, J. a. Cruz, J. Lucas, and R. Pascal, "Wave Powered Desalination," in *Proceedings of the International Conference on Integrated Sustainable Energy Resources in Arid Regions*, Abu Dhabi, 2007.

[5] J. Lucas, J. a. Cruz, S. H. Salter, and J. Taylor, "Update on the Design of a 1:33 Scale Model of a Modified Edinburgh Duck WEC," in *27th International Conference on Offshore Mechanics and Arctic Engineering*, Jun. 2008.

[6] J. Lucas, S. H. Salter, J. a. Cruz, and J. Taylor, "Performance optimisation of a modified Duck through optimal mass distribution," in *Proceedings of the 8th European Wave and Tidal Energy Conference*, Uppsala, Sweden, 2009, pp. 270–279.

[7] J.-B. Saulnier, A. Clément, A. F. D. O. Falcão, T. Pontes, M. Prevosto, and P. Ricci, "Wave groupiness and spectral bandwidth as relevant parameters for the performance assessment of wave energy converters," *Ocean Engineering*, vol. 38, pp. 130–147, Nov. 2010. [Online]. Available: http://linkinghub.elsevier.com/retrieve/pii/S0029801810002179

[8] M. J. Tucker and E. G. Pitt, *Waves in Ocean engineering*. Elsevier, 2001.

[9] R. Pascal and I. Bryden, "Directional spectrum methods for deterministic waves," *Ocean engineering*, vol. submited, 2011.

[10] R. Pascal, J. Lucas, D. Ingram, and I. Bryden, "Assessing and Improving the Edinburgh Curved Wave Tank," in *Proceedings of the 19th International Offshore and Polar Engineering Conference*, Osaka, Jun. 2009.

[11] M. Crawley, *The R book*. John Wiley & Sons Inc, 2007.

[12] R Development Core Team, "R: A Language and Environment for Statistical Computing," Vienna, Austria, 2009. [Online]. Available: http://www.r-project.org